Chemical Science

RSC Publishing

EDGE ARTICLE

View Article Online
View Journal | View Issue

Cite this: *Chem. Sci.*, 2013, **4**, 2054

Selective adsorption of ethylene over ethane and propylene over propane in the metal–organic frameworks M_2(dobdc) (M = Mg, Mn, Fe, Co, Ni, Zn)†

Stephen J. Geier,[a] Jarad A. Mason,[a] Eric D. Bloch,[a] Wendy L. Queen,[bc] Matthew R. Hudson,[c] Craig M. Brown[cd] and Jeffrey R. Long*[ae]

Received 4th January 2013
Accepted 25th February 2013

DOI: 10.1039/c3sc00032j

www.rsc.org/chemicalscience

A significant reduction in the energy costs associated with the cryogenic separation of ethylene–ethane and propylene–propane mixtures could potentially be realized through the use of selective solid adsorbents that operate at higher temperatures. The metal–organic frameworks M_2(dobdc) (M = Mg, Mn, Fe, Co, Ni, Zn; dobdc^{4-} = 2,5-dioxido-1,4-benzenedicarboxylate) are of particular interest for this application, owing to their high density of coordinatively unsaturated M^{2+} cation sites that can selectively interact with unsaturated hydrocarbons. Here, we present gas adsorption data for ethylene, ethane, propylene, and propane at 45, 60, and 80 °C for the entire series. The means of sample preparation and activation is found to be important for achieving high separation selectivities and capacities. While all of the compounds investigated show good performance characteristics, Fe_2(dobdc) and Mn_2(dobdc) exhibit the highest selectivities for the separation of ethylene–ethane and propylene–propane mixtures, respectively. Crystal structures determined from neutron powder diffraction data elucidate the binding of ethane, ethylene, and propylene in Mn_2(dobdc) and Co_2(dobdc).

Introduction

Separations of ethylene–ethane and propylene–propane mixtures are important industrial processes currently carried out at an enormous scale. To date, the most commonly employed method for the commercial separation of small hydrocarbons is cryogenic distillation, a process that is extremely cost intensive in terms of both capital and energy input, due primarily to the low temperatures and high pressures required.[1] Replacing large-scale cryogenic distillation with higher-temperature separation processes could potentially save tremendous amounts of energy. Among these are separation processes that take advantage of selective chemical interactions with carbon–carbon double bonds, such as the absorptive separations involving complexation of Cu^+ or Ag^+ ions with olefin molecules in solution.[2] Such systems are generally somewhat inefficient, however, due to the poor contact between the hydrocarbons and the liquid absorbent. In addition, heating the solution of metal ions to liberate the absorbed olefin molecules can also require significant energy input. Accordingly, porous solid adsorbents, which could potentially result in a much lower regeneration energy, have also been investigated.[3–6] While cryogenic distillation relies on small differences in the boiling points of the components of olefin–paraffin mixtures, adsorptive separations take advantage of other dissimilar physical properties such as kinetic diameter, dipole moment (μ), quadrupole moment (Θ), and polarizability (α) (see Table 1).

Metal–organic frameworks are a relatively new class of microporous materials that have received considerable recent attention for the adsorptive separation of gas mixtures.[6] Of the multitude of structures reported over the past decade, among

[a]*Department of Chemistry, University of California, Berkeley, CA 94720, USA. E-mail: jrlong@berkeley.edu*

[b]*The Molecular Foundry, Lawrence Berkeley National Laboratory, Berkeley, CA 94720, USA*

[c]*Center for Neutron Research, National Institute of Standards and Technology, Gaithersburg, MD 20899, USA*

[d]*Department of Chemical Engineering, University of Delaware, Newark, DE 19716, USA*

[e]*Materials Sciences Division, Lawrence Berkeley National Laboratory, Berkeley, CA 94720, USA*

† Electronic supplementary information (ESI) available: Synthesis and activation procedures, calculations, fitting parameters, gas adsorption data, tables of structural refinement details, and additional figures. See DOI: 10.1039/c3sc00032j

Table 1 Relevant physical properties of C_1–C_3 hydrocarbons[7]

Gas	Kinetic diameter (Å)	Boiling point (K)	μ ($\times 10^{-30}$ C m)	Θ ($\times 10^{40}$ C m^2)	α (10^{-25} cm^3)
CH_4	3.758	109–113	0	0	25.93
C_2H_6	4.4443	184.5	0	2.17	44.3–44.7
C_2H_4	4.163	169.4	0	5.00	42.52
C_3H_8	4.3–5.118	231.1	0.28	0	62.9–63.7
C_3H_6	4.678	225.4	1.22	0	62.6

the most studied has been M_2(dobdc) (dobdc^{4-} = 2,5-dioxido-1,4-benzenedicarboxylate). This framework, also commonly referred to as MOF-74, CPO-27, or M_2(dhtp), features a hexagonal array of one-dimensional channels lined with five-coordinate M^{2+} ions, each possessing an open coordination site. Significantly, the use of the compact tetraanionic bridging ligand dobdc^{4-} endows this material with an extraordinarily high density of coordinatively unsaturated metal cation surface sites. These have been shown to serve as strongly polarizing sites for gas molecules, which has motivated investigations of possible applications in the storage of H_2,[7,8] CH_4,[8a,9] and acetylene,[10] as well as CO_2–N_2,[11] CO_2–H_2,[12] O_2–N_2,[13] CO_2–CH_4,[14] and, very recently, paraffin–olefin separations.[15] An interesting characteristic of the structure type is the fact that an isostructural series of frameworks can be obtained with M = Mg, Mn, Fe, Co, Ni, and Zn,[11,13,16] which enables the study of how properties change with variation of just the framework metal cation. While series of isostructural frameworks are also known for other materials such as M_2(btc)$_3$ (M = Cr, Fe, Ni, Cu, Zn, Mo, Ru; btc^{3-} = 1,3,5-benzenetricarboxylate)[17] and $M_3[(M_4Cl)_3(BTT)_8]_2$ (M = Mn, Fe, Co, Cu, Cd; BTT^{3-} = benzene-1,3,5-tristetrazolate)[18] structure types, these materials ultimately have lower separation capacities and further, owing to lower thermal stability, often cannot be completely desolvated without collapse of the framework.

Several reports have recently emerged demonstrating the potential use of M_2(dobdc) compounds in the separation of small hydrocarbons,[15] but a complete analysis of the adsorption and separation of C_2 and C_3 olefins and paraffins with these materials is lacking. Here, adsorption isotherms, isosteric heats of adsorption, ideal adsorbed solution theory (IAST) selectivities, and molecular structures are evaluated to assess the utility of the various members of this isostructural series for ethylene–ethane and propylene–propane separations.

Results and discussion

Hydrocarbon adsorption isotherms

In order to evaluate the performance of all six isostructural M_2(dobdc) (M = Mg, Mn, Fe, Co, Ni, Zn) compounds for ethylene–ethane and propylene–propane separations, single-component gas adsorption isotherms were measured for each metal (note that the Fe data was taken from our previous work)[15e] and hydrocarbon at 45, 60, and 80 °C (Fig. 1 and S2–S6†). Regardless of the metal, the uptake of saturated hydrocarbons increases with polarizablity (methane[16e] < ethane < propane) due to increasing charge-induced dipole interactions with the exposed cations. While polarizability is an important factor in unsaturated hydrocarbon adsorption, the electron donating and accepting properties of the metal center must also be considered. Specifically, metals more capable of accepting π electron density and/or donating electron density into the empty π^* orbital of the olefin are expected to show a stronger interaction.[2,3a,15]

Although these frameworks have the same three-dimensional structure, the different masses of the metals make a direct comparison of their gravimetric adsorption isotherms cumbersome. To show the differences between frameworks more clearly, the adsorption isotherms for all hydrocarbons at 45 °C are plotted in Fig. 1 as a function of the amount adsorbed per M rather than per gram of adsorbent. With the exception of Mg_2(dobdc), the capacity for ethane and propane at 1 bar is similar for each metal, approaching 0.8 and 0.9 molecules adsorbed per M atom, respectively. The lower capacities for Mg_2(dobdc) are likely an indication that some Mg^{2+} sites are not accessible, which could be due to incomplete activation, a large number of defects, or the presence of an amorphous phase. These differences are not obvious when plotting the adsorption isotherms on a gravimetric basis (mmol g^{-1}) because of the much lower molecular weight of Mg_2(dobdc).

In all cases, the amount of ethylene or propylene adsorbed is greater than that of ethane or propane over the entire pressure range measured, from 0 to 1 bar. Significantly, this demonstrates that all six M_2(dobdc) frameworks have potential for separating mixtures of paraffins and olefins and warrant further study. Indeed, the Fe, Mn, and Co analogues all have ethylene capacities approaching 1 molecule adsorbed per M atom, while with the exception of Mg_2(dobdc), the propylene capacity is similar for each metal, approaching 1.1 molecules adsorbed per M atom.

Since ethylene or propylene would be selectively retained by each material in an actual separation, the capacities for these gases will be important for determining the best adsorbent to use in a particular process (Tables S14 and S15†). Here, Mn_2(dobdc) and Mg_2(dobdc) have the highest gravimetric capacities at 1 bar for ethylene (6.3 mmol g^{-1}) and propylene (7.5 mmol g^{-1}), respectively. For a fixed bed adsorber, it is also important to consider volumetric capacity, as this will determine the size of bed necessary to capture a given amount of gas.[19] In contrast to gravimetric capacity, the volumetric capacity is highest in Ni_2(dobdc) for both ethylene (7.3 mmol cm^{-3}) and propylene (8.4 mmol cm^{-3}). It is important to note that the volumetric capacities are calculated using the ideal crystallographic densities of each framework. In order to properly compare the capacities for a realistic application, differences in the effective packing densities of each material must be fully evaluated. Nonetheless, these results demonstrate the importance of fully characterizing the adsorption properties of the entire M_2(dobdc) series since different metals may be preferred depending on the relative importance of maximizing volumetric or gravimetric capacity.

Importance of sample preparation and activation

As we have previously shown for MOF-5, the preparation and handling of metal–organic frameworks can have a tremendous impact on their gas adsorption properties.[20] To compare different frameworks objectively for the separation of various gas mixtures, it is important to try to ensure their optimal synthesis and complete activation. Although a number of investigations into the hydrocarbon separation performance of several M_2(dobdc) analogues have been reported,[15] it is difficult to directly compare the results due to potential differences in sample preparation and activation. For example, an early study

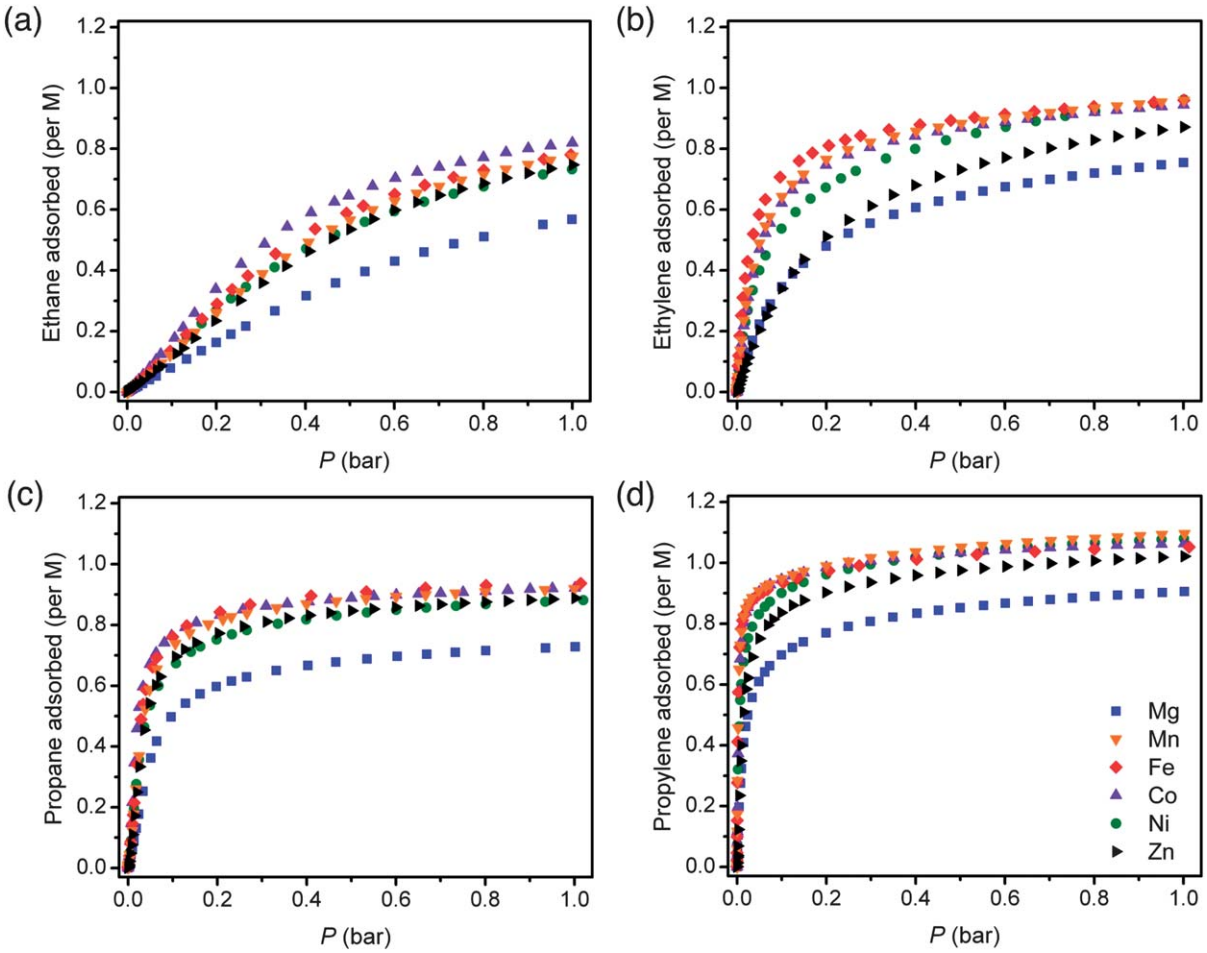

Fig. 1 Equilibrium excess adsorption isotherms for ethane (a), ethylene (b), propane (c), and propylene (d) in M_2(dobdc) at 45 °C. Note that the amount adsorbed is plotted in terms of hydrocarbon molecules per M atom.

by Matzger and coworkers measured ethane and ethylene adsorption in Co_2(dobdc), Ni_2(dobdc), and Zn_2(dobdc) at 25 °C.[15a] All three materials adsorbed between 5.4 and 7.9 mmol g^{-1} of either hydrocarbon under these conditions. As expected, and in good agreement with the results presented here, all three frameworks adsorbed more ethylene than ethane at this temperature. The Co and Zn frameworks adsorbed 0.5 and 0.7 mmol g^{-1} more ethylene than ethane. The Ni framework, however, showed a surprising 2.5 mmol g^{-1} difference in uptake. Interestingly, in the ethylene–ethane and propylene–propane isotherms reported for various M_2(dobdc) frameworks, there are very few cases in which the adsorption of an unsaturated hydrocarbon is more than 1.5 mmol g^{-1} higher than its saturated counterpart. This may suggest an incomplete removal of adsorbed ethylene during regeneration before the ethane measurement was performed, which would lead to an erroneously low ethane isotherm and too high of a predicted selectivity.

Deng and coworkers recently reported the ethylene–ethane and propylene–propane uptake capacities and selectivities of Mg_2(dobdc) at 5, 25, and 45 °C.[15b] While these results are quite similar to ours, in which, at a given temperature, hydrocarbon uptakes at 1 bar generally follow the trend ethane < propane < ethylene < propylene, other recent reports present conflicting data. For example, in Co_2(dobdc) at both 0 and 23 °C, He and coworkers report uptakes of propane and propylene that are over 1.5 mmol g^{-1} smaller than ethane and ethylene.[15d] This does not appear to be simply a product of incomplete sample activation as the ethane and ethylene capacities at 25 °C match quite closely to the results from Matzger and coworkers.[15a] Furthermore, the reported Langmuir surface area of 1450 m^2 g^{-1} for Co_2(dobdc) is in good agreement with numerous values previously reported for this framework and with the surface area reported here. The anomalously low propane and propylene uptake may simply be a result of experimental error or incomplete hydrocarbon desorption between experiments.

Inconsistencies in reported isotherms may in some cases be due to dramatic differences in reported surface areas of the materials employed in the adsorption measurements. Samples of M_2(dobdc) with lower surface areas will likely have fewer accessible vacant metal coordination sites, whether a result of pore blockage or partial occupation of the metal sites by unreacted ligand or solvent molecules. Given that the primary binding site is the exposed metal cation, lower surface area materials are expected to show lower hydrocarbon uptake. For example, the recent paper by Bae and coworkers discusses the

separation of propylene–propane mixtures with Mg_2(dobdc), Mn_2(dobdc), and Co_2(dobdc).[15c] For the Mg and Mn compounds, gas uptakes are significantly less than those reported both here and by Deng and coworkers.[15b] Indeed, Fig. S11† compares the adsorption of propane and propylene at 25 °C in a sample of Mn_2(dobdc) exhibiting a Langmuir surface area of 1284 $m^2\ g^{-1}$ (ref. 15*c*) to our data, collected at 45 °C employing a sample with a Langmuir surface area of 1797 $m^2\ g^{-1}$. Despite collecting the data at a much higher temperature, we observe a significantly higher capacity for each gas. It is clear that, in order to properly evaluate and compare the performance of these metal–organic frameworks, any bias caused by inconsistencies in the synthesis or incomplete activation must be minimized.

Isosteric heats of adsorption

In an initial attempt to assess the potential of each material for ethylene–ethane and propylene–propane separations, isosteric heats of adsorption, Q_{st}, were calculated as a function of loading using the adsorption isotherms at 45, 60, and 80 °C. Here, a dual-site Langmuir–Freundlich equation (eqn (1)) was used to independently fit every adsorption isotherm at each temperature, T, where n is the absolute amount adsorbed in mmol g^{-1}, P is the pressure in bar, $q_{sat,i}$ are the saturation capacities in mmol g^{-1}, b_i are the Langmuir parameter in bar^{-1}, and ν_i are the Freundlich parameters for two sites a and b.

$$n = \frac{q_{sat,a} b_a P^{\nu_a}}{1 + b_a P^{\nu_a}} + \frac{q_{sat,b} b_b P^{\nu_b}}{1 + b_b P^{\nu_b}} \quad (1)$$

Recent work has demonstrated the ability of the dual-site Langmuir–Freundlich equation to accurately describe adsorption in metal–organic frameworks with strong binding sites.[13,19,21] A complete description of the isosteric heat calculations and tables of fitted parameters can be found in the ESI.† Calculating the isosteric heat of adsorption was not possible for ethylene adsorption in Ni_2(dobdc) due to a slight hysteresis observed in the 45 °C adsorption isotherm. A similar hysteresis was previously observed by Matzger and coworkers.[15a] Since some nickel(II) species are known ethylene polymerization catalyst precursors,[22] the small amount of irreversible ethylene adsorption could be a result of some Ni^{2+} sites in the framework showing unusually high reactivity. Further studies into the reactivity of Ni_2(dobdc) towards ethylene activation are underway.

After using the isotherm fits to solve for equilibrium pressures that correspond to the same adsorbate loading at each temperature, the Clausius–Clapeyron equation (eqn (2)) can be employed to determine the isosteric heat of adsorption for a given amount adsorbed.

$$\ln P = -\frac{Q_{st}}{R}\left(\frac{1}{T}\right) + C \quad (2)$$

Specifically, a line is fit to a plot of $1/T$ *vs.* $\ln P$ for each loading, with the slope affording $-Q_{st}/R$. An error in the isosteric heat for a given loading can be calculated from the standard error in the slope of the best-fit line. Fundamentally, this error describes the quality of agreement between the fitted isotherms and the Clausius–Clapeyron relation. It is important to note that the Clausius–Clapeyron equation assumes that the isosteric heat of adsorption does not vary with temperature. This is generally true over a narrow temperature range, but could lead to larger errors when a wide temperature range is used, even with high quality adsorption data and accurate isotherm fits.

The isosteric heats of adsorption as a function of loading are plotted for each metal and hydrocarbon in Fig. S7.† It is important to note that the heat of adsorption is influenced by both framework–hydrocarbon and hydrocarbon–hydrocarbon interactions, making direct comparisons between the different isosteric heats of adsorption curves challenging. Intermolecular interactions appear to be particularly significant for ethane and propane, as evidenced by the steady increase in $-Q_{st}$ with loading, which is consistent for all metals. This trend was also observed in a previous study of hydrocarbon adsorption in Mg_2(dobdc).[15b]

To better compare the different binding affinities for the hydrocarbons in each M_2(dobdc) analogue, the isosteric heats of adsorption are plotted at a loading of 1 hydrocarbon molecule per 6 M atoms, since intermolecular interactions are expected to have a smaller contribution to the overall isosteric heat at low surface coverage (Fig. 2). Although comparing the binding strengths of each hydrocarbon across the series of exposed metal cation sites is difficult owing to the relatively small differences in the values and the size of the error bars, there are several important trends worth noting. As expected, $-Q_{st}$ increases consistently for each metal with ethane < propane < ethylene < propylene. This is due to the greater polarizability of C_3 hydrocarbons relative to C_2 hydrocarbons and to the interaction of the exposed metal cations with the olefin π bond. Significantly, all six materials show much greater affinities for unsaturated C_2 or C_3 hydrocarbons than saturated, with differences in isosteric heats of adsorption between

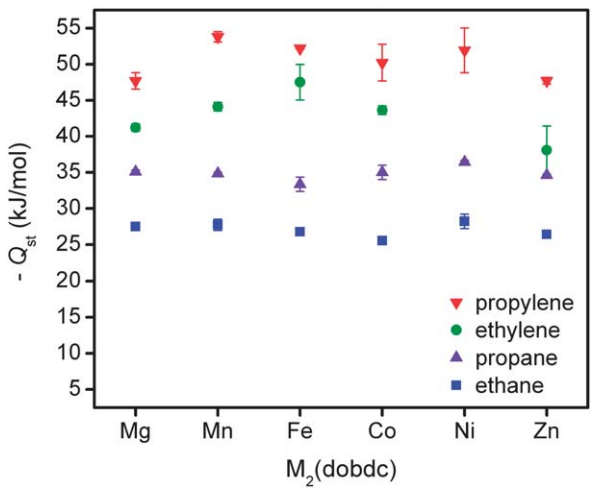

Fig. 2 Isosteric heats of adsorption at a loading of 1 hydrocarbon molecule per 6 M atoms for propylene (red), ethylene (green), propane (purple), and ethane (blue). Error bars are determined from fitting to the Clausius–Clapeyron equation.

10–20 kJ mol^{-1}. Interestingly, the strongest interaction with ethylene is observed for M = Fe, and does not appear to be a simple function of the charge density at the exposed M^{2+} ion. Perhaps more surprising, the large Mn^{2+} ion shows the highest affinity for propylene, although the $-Q_{st}$ observed for M = Ni is within error.

IAST selectivities

The significant differences in isosteric heats of adsorption suggest that highly selective olefin–paraffin separations are feasible with these materials. Since binary gas adsorption isotherms cannot be conveniently and rapidly measured, it is necessary to use an adsorption model, such as ideal adsorbed solution theory (IAST), to predict mixed gas behavior from experimentally measured single-component isotherms. The accuracy of the IAST procedure has already been established for a wide variety of gas mixtures in different zeolites[23] and metal–organic frameworks.[21a,c] Here, IAST is used to estimate the ethylene–ethane and propylene–propane selectivities for all six frameworks. An alkene–alkane selectivity factor, S, can be calculated using the dual-site Langmuir–Freundlich fits and eqn (3), where n is the amount of each component adsorbed as determined from IAST and x is the mole fraction of each component in the gas phase at equilibrium.

$$S = \frac{n_{\text{alkene}}/n_{\text{alkane}}}{x_{\text{alkene}}/x_{\text{alkane}}} \quad (3)$$

Since the exact composition of the olefin–paraffin mixture may vary significantly depending on the application, the ethylene–ethane and propylene–propane IAST selectivities at 45 °C and a total pressure of 1 bar are calculated over a range of compositions (Fig. 3). For all M_2(dobdc) compounds, the resulting selectivity is higher for propylene–propane than for ethylene–ethane. The Mg and Zn analogues exhibit the lowest IAST selectivities for both separations, which is primarily due to the weaker interactions between these metal cations and the unsaturated hydrocarbons. While Fe_2(dobdc) has the highest selectivity for ethylene–ethane at all mixture compositions, Mn_2(dobdc) shows the greatest selectivity for propylene–propane. Note that the propylene–propane selectivity increases for mixtures with greater propylene content, while the ethylene–ethane selectivity decreases or is unchanged regardless of the composition.

Crystal structures

Powder neutron diffraction experiments were carried out to investigate the nature of the interaction of adsorbed hydrocarbon molecules with the accessible metal cation sites in selected M_2(dobdc) compounds. Owing to their crystalline nature, experiments of this type are frequently used to characterize the local structures associated with metal–adsorbate interactions in metal–organic frameworks. For example, *in situ* neutron diffraction experiments have recently been utilized to reveal the binding of D_2,[21d] N_2,[13] O_2,[13] and C_2/C_3 hydrocarbons[15e] to the Fe^{2+} ions in Fe_2(dobdc). Here, substoichiometric equivalents of deuterated ethane, ethylene, or propylene (Table S17†) were dosed into activated samples of Mn_2(dobdc) and Co_2(dobdc) at room temperature. To minimize thermal distortions, the hydrocarbon-dosed samples were slowly cooled to 10 K for data collection. Rietveld refinements performed against these datasets led to the structural models presented in Tables S18–S25; full refinement details are available in the ESI.† As is suggested by the isotherm data, in which saturation capacities approach one molecule per metal center, the strongest binding sites in these materials are confirmed through the neutron diffraction data to be at the exposed metal cation sites.

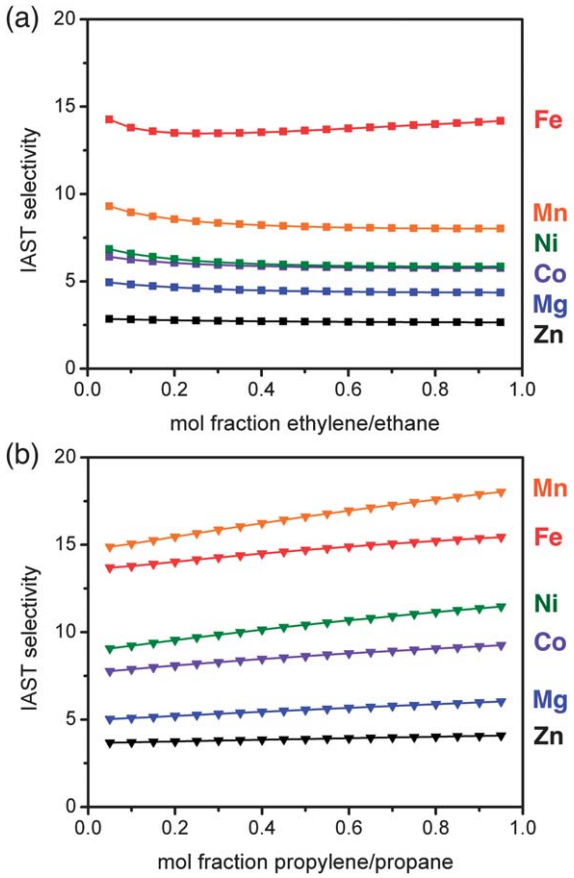

Fig. 3 Ideal adsorbed solution theory (IAST) selectivities for mixtures of ethylene–ethane (top) and propylene–propane (bottom) of varying compositions at 45 °C and a total pressure of 1 bar.

The structure of desolvated Mn_2(dobdc), reported here for the first time, shows a significant distortion in the square pyramidal geometry at the metal center. While the Mn atom lies in the plane created by the four equatorial O atoms, O–Mn–O bond angles vary widely from 74(1)° to 111(1)° and Mn–O bond lengths range from 1.94(3) to 2.27(2) Å within this plane (Fig. S10†). The axial Mn–O bond lies at an angle of approximately 80° from the plane of the equatorial oxygen atoms. Interestingly, the structural models developed for Mn_2(dobdc) dosed with ethane, ethylene, or propylene show anomalously long Mn–hydrocarbon interactions, which could be an artifact of the structural model not adequately accounting for framework disorder. Nonetheless, in the case of ethane adsorbed

within Mn_2(dobdc), a clear secondary binding site is apparent in the center of the hexagonal channels of the framework (Fig. 4). Significantly, this is the first time such a site has been observed. Most likely this is a result of the larger pores in Mn_2(dobdc), associated with the larger ionic radius of the Mn^{2+} ions, which lead to a more efficient hydrocarbon packing.

Rietveld refinements against data collected upon dosing hydrocarbons in Co_2(dobdc) afforded the structure fragments depicted at the bottom of Fig. 4. For ethane, only one adsorption site is apparent, with Co–D distances of 2.34(4) Å and 2.50(4) Å. We note that these are slightly shorter than the analogous Fe–D distances of 2.59(2) Å in Fe_2(dobdc),[15e] despite a similar isosteric heat of adsorption. It is worthwhile to note that crystal structures of transition metal–alkane σ-complexes are rare with the only other examples being our previously reported Fe_2(dobdc)–ethane and –propane structures,[15e] and iron(II)–heptane,[24] rhodium(I)–norbornane[25] and uranium(III)–methylcyclohexane complexes.[26]

The unsaturated hydrocarbons ethylene and propylene bind the Co^{2+} ions in Co_2(dobdc) in the expected side-on fashion, with Co–C distances of 2.60(4) Å and 2.66(5)/2.73(6) Å, respectively. Despite the existence of several well-known cobalt(II) polymerization catalyst precursors, to the best of our knowledge, these represent the first structures determined for ethylene or propylene bound to a Co^{2+} ion. The Co–C distances observed here are much longer than those observed in cobalt(I)–ethylene complexes (1.908–2.055 Å),[27] a cobalt(III)–ethylene complex (2.034–2.040 Å),[28] and a cobalt(−1)–ethylene complex (2.007–2.039 Å).[29] The major differences here are consistent with the high-spin nature of the cobalt(II) centers in Co_2(dobdc), as enforced by the weak ligand field of the five oxo donor ligands, which leads to an essentially ionic interaction with little to no π-backbonding. The longer metal–olefin bond lengths for Co_2(dobdc) compared to the Fe–C distances of 2.42(2) Å for ethylene and 2.56(2)/2.60(2) Å for propylene in Fe_2(dobdc) are consistent with the lower magnitudes of the Q_{st} values of −43.6 kJ mol^{-1} for ethylene and −50.2 kJ mol^{-1} for propylene compared to the respective values of −47.5 and −52.2 kJ mol^{-1} in Fe_2(dobdc). These results are further consistent with the lower IAST selectivities of Co_2(dobdc).

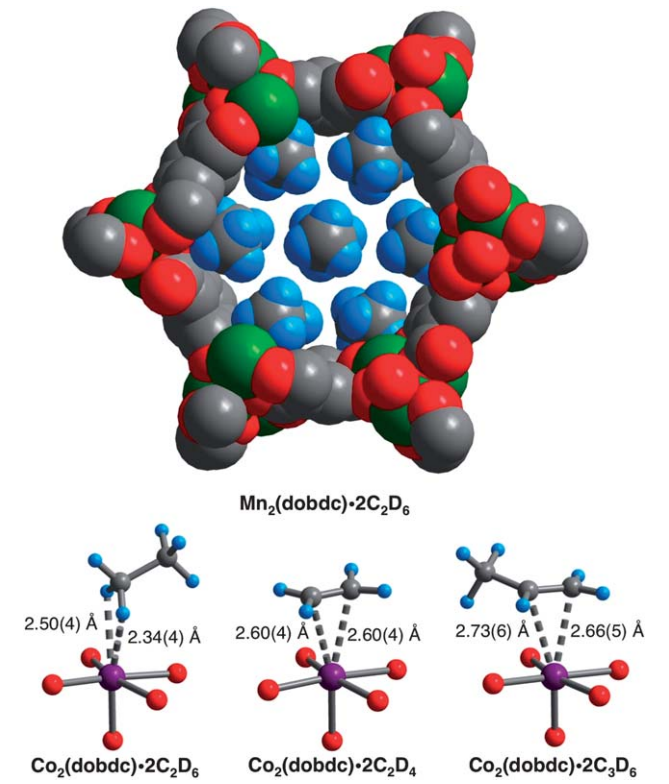

Fig. 4 Upper: a portion of the crystal structure of Mn_2(dobdc)·$2C_2D_6$, as determined by powder neutron diffraction. Lower: first coordination sphere for the cobalt centers upon dosing Co_2(dobdc) with ethane, ethylene, and propylene; green, red, gray, light blue, and purple represent Mn, O, C, D, and Co atoms, respectively. Values in parentheses indicate one standard deviation in the refined intermolecular distances.

Conclusions

The foregoing results demonstrate the potential utility of the M_2(dobdc) frameworks in ethylene–ethane and propylene–propane separations. Owing to their high density of exposed metal cations and the preferential interaction that these sites have with unsaturated hydrocarbons over saturated, all frameworks studied here have high ethylene and propylene capacities and promising IAST selectivities. In determining the best framework for an actual separation process, other factors such as cost, recyclability, stability, processability, and environmental impact will also need to be considered.

Acknowledgements

This research was funded through the Center for Gas Separations Relevant to Clean Energy Technologies, an Energy Frontier Research Center funded by the U.S. Department of Energy, Office of Science, Office of Basic Energy Sciences under Award no. DE-SC0001015. We thank the Camille and Henry Dreyfus Foundation Postdoctoral Program in Environmental Chemistry and NSERC for support of S. J. G., the National Science Foundation for fellowship support of J. A. M, and support for W. L. Q. and M. R. H. from the NIST/NRC Fellowship Program.

Notes and references

1 R. B. Eldrige, *Ind. Eng. Chem. Res.*, 1993, **32**, 2208–2212.
2 D. J. Safarik and R. B. Eldridge, *Ind. Eng. Chem. Res.*, 1998, **37**, 2571–2581.
3 (*a*) S. U. Rege, J. Padin and R. T. Yang, *AIChE J.*, 1998, **44**, 799–809; (*b*) J. Padin, S. U. Rege, R. T. Yang and L. S. Cheng, *Chem. Eng. Sci.*, 2000, **55**, 4525–4535; (*c*) J. Kim, L.-C. Lin, R. L. Martin, J. A. Swisher, M. Haranczyk and B. Smit, *Langmuir*, 2012, **28**, 11914–11919.
4 (*a*) K. Li, D. H. Olson, J. Seidel, T. J. Emge, H. Gong, H. Zeng and J. Li, *J. Am. Chem. Soc.*, 2009, **131**, 10368–10369; (*b*) H. Bux, C. Chmelik, R. Krishna and J. Caro, *J. Membr. Sci.*, 2011, **369**, 284–289.

5 C. Y. Lee, Y. S. Bae, N. C. Jeong, O. K. Farha, A. A. Sarjeant, C. L. Stern, P. Nickias, R. Q. Snurr, J. T. Hupp and S. T. Nguyen, *J. Am. Chem. Soc.*, 2011, **133**, 5228–5231.

6 (*a*) M. Eddaoudi, J. Kim, N. Rosi, D. Vodak, J. Wachter, M. O'Keeffe and O. M. Yaghi, *Science*, 2002, **295**, 469–472; (*b*) S. Kitagawa, R. Kitaura and S.-i. Noro, *Angew. Chem., Int. Ed.*, 2004, **43**, 2334–2375; (*c*) H. K. Chae, D. Y. Siberio-Perez, J. Kim, Y. B. Go, M. Eddaoudi, A. J. Matzger, M. O'Keeffe and O. M. Yaghi, *Nature*, 2004, **427**, 523–527; (*d*) A. R. Millward and O. M. Yaghi, *J. Am. Chem. Soc.*, 2005, **127**, 17998–17999; (*e*) H. Furukawa, M. A. Miller and O. M. Yaghi, *J. Mater. Chem.*, 2007, **17**, 3197–3204; (*f*) G. Ferey, *Chem. Soc. Rev.*, 2008, **37**, 191–214; (*g*) J. D. Figueroa, T. Fout, S. Plasynski, H. McIlvried and R. D. Srivastava, *Int. J. Greenhouse Gas Control*, 2008, **2**, 9–20; (*h*) D. Britt, H. Furukawa, B. Wang, T. G. Glover and O. M. Yaghi, *Proc. Natl. Acad. Sci. U. S. A.*, 2009, **106**, 20637–20640; (*i*) L. J. Murray, M. Dincă and J. R. Long, *Chem. Soc. Rev.*, 2009, **38**, 1294–1314; (*j*) D. M. D'Alessandro, B. Smit and J. R. Long, *Angew. Chem., Int. Ed.*, 2010, **49**, 6058–6082; (*k*) G. Ferey, C. Serre, T. Devic, G. Maurin, H. Jobic, P. L. Llewellyn, W. G. De, A. Vimont, M. Daturi and J.-S. Chang, *Chem. Soc. Rev.*, 2011, **40**, 550–562; (*l*) J. M. Simmons, H. Wu, W. Zhou and T. Yildirim, *Energy Environ. Sci.*, 2011, **4**, 2177–2185; (*m*) J.-R. Li, J. Sculley and H.-C. Zhou, *Chem. Rev.*, 2012, **112**, 869–932; (*n*) R. E. Morris and P. S. Wheatley, *Angew. Chem., Int. Ed.*, 2008, **47**, 4966–4981; (*o*) K. Sumida, D. L. Rogow, J. A. Mason, T. M. McDonald, E. D. Bloch, Z. R. Herm, T.-H. Bae and J. R. Long, *Chem. Rev.*, 2012, **112**, 724–781; (*p*) Y. He, W. Zhou, R. Krishna and B. Chen, *Chem. Commun.*, 2012, **48**, 11813–11831; (*q*) S.-C. Xiang, Z. Zhang, C.-G. Zhao, K. Hong, X. Zhao, D.-R. Ding, M.-H. Xie, C.-D. Wu, M. C. Das, R. Gill, K. M. Thomas and B. Chen, *Nat. Commun.*, 2011, **2**, 204; (*r*) M. C. Das, Q. Guo, Y. He, J. Kim, C.-G. Zhao, K. Hong, S. Xiang, Z. Zhang, K. M. Thomas, R. Krishna and B. Chen, *J. Am. Chem. Soc.*, 2012, **134**, 8703–8710.

7 J.-R. Li, R. J. Kuppler and H.-C. Zhou, *Chem. Soc. Rev.*, 2009, **38**, 1477–1504.

8 (*a*) N. L. Rosi, J. Eckert, M. Eddaoudi, D. T. Vodak, J. Kim, M. O'Keeffe and O. M. Yaghi, *Science*, 2003, **300**, 1127–1130; (*b*) J. G. Vitillo, L. Regli, S. Chavan, G. Ricchiardi, G. Spoto, P. D. C. Dietzel, S. Bordiga and A. Zecchina, *J. Am. Chem. Soc.*, 2008, **130**, 8386–8396; (*c*) P. D. C. Dietzel, P. A. Georgiev, J. Eckert, R. Blom, T. Strässle and T. Unruh, *Chem. Commun.*, 2010, **46**, 4962–4964.

9 S. Kitagawa, R. Kitaura and S.-i. Noro, *Angew. Chem., Int. Ed.*, 2004, **43**, 2334–2375.

10 (*a*) S. Xiang, W. Zhou, Z. Zhang, M. A. Green, Y. Liu and B. Chen, *Angew. Chem., Int. Ed.*, 2010, **49**, 4615–4618, S4615/4611–S4615/4617; (*b*) Z. Zhang, S. Xiang and B. Chen, *CrystEngComm*, 2011, **13**, 5983–5992; (*c*) S. M. Chavan, G. C. Shearer, E. Bloch and S. Bordiga, *ChemPhysChem*, 2012, **13**, 445–448.

11 S. R. Caskey, A. G. Wong-Foy and A. J. Matzger, *J. Am. Chem. Soc.*, 2008, **130**, 10870–10871.

12 Z. R. Herm, J. A. Swisher, B. Smit, R. Krishna and J. R. Long, *J. Am. Chem. Soc.*, 2011, **133**, 5664–5667.

13 E. D. Bloch, L. J. Murray, W. L. Queen, S. Chavan, S. N. Maximoff, J. P. Bigi, R. Krishna, V. K. Peterson, F. Grandjean, G. J. Long, B. Smit, S. Bordiga, C. M. Brown and J. R. Long, *J. Am. Chem. Soc.*, 2011, **133**, 14814–14822.

14 P. D. C. Dietzel, V. Besikiotis and R. Blom, *J. Mater. Chem.*, 2009, **19**, 7362–7370.

15 (*a*) A. J. Matzger, A. G. Wong-Foy and S. Caskey, *US Pat.*, US 2010/0258004, A1, 2010; (*b*) Z. Bao, S. Alnemrat, L. Yu, I. Vasiliev, Q. Ren, X. Lu and S. Deng, *Langmuir*, 2011, **27**, 13554–13562; (*c*) Y.-S. Bae, C. Y. Lee, K. C. Kim, O. K. Farha, P. Nickias, J. T. Hupp, S. T. Nguyen and R. Q. Snurr, *Angew. Chem., Int. Ed.*, 2012, **51**, 1857–1860; (*d*) Y. He, R. Krishna and B. Chen, *Energy Environ. Sci.*, 2012, **5**, 9107–9120; (*e*) E. D. Bloch, W. L. Queen, R. Krishna, J. M. Zadrozny, C. M. Brown and J. R. Long, *Science*, 2012, **335**, 1606–1610.

16 (*a*) N. L. Rosi, J. Kim, M. Eddaoudi, B. Chen, M. O'Keeffe and O. M. Yaghi, *J. Am. Chem. Soc.*, 2005, **127**, 1504–1518; (*b*) P. D. C. Dietzel, Y. Morita, R. Blom and H. Fjellvåg, *Angew. Chem., Int. Ed.*, 2005, **44**, 6354–6358; (*c*) P. D. C. Dietzel, B. Panella, M. Hirscher, R. Blom and H. Fjellvag, *Chem. Commun.*, 2006, 959–961; (*d*) P. D. C. Dietzel, R. Blom and H. Fjellvaag, *Eur. J. Inorg. Chem.*, 2008, 3624–3632; (*e*) H. Wu, W. Zhou and T. Yildirim, *J. Am. Chem. Soc.*, 2009, **131**, 4995–5000.

17 (*a*) S. S.-Y. Chui, S. M.-F. Lo, J. P. H. Charmant, A. G. Orpen and I. D. Williams, *Science*, 1999, **283**, 1148–1150; (*b*) M. Kramer, U. Schwarz and S. Kaskel, *J. Mater. Chem.*, 2006, **16**, 2245–2248; (*c*) L. J. Murray, M. Dincă, J. Yano, S. Chavan, S. Bordiga, C. M. Brown and J. R. Long, *J. Am. Chem. Soc.*, 2010, **132**, 7856–7857; (*d*) J. I. Feldblyum, M. Liu, D. W. Gidley and A. J. Matzger, *J. Am. Chem. Soc.*, 2011, **133**, 18257–18263; (*e*) O. Kozachuk, K. Yusenko, H. Noei, Y. Wang, S. Walleck, T. Glaser and R. A. Fischer, *Chem. Commun.*, 2011, **47**, 8509–8511.

18 (*a*) M. Dincă, A. Dailly, Y. Liu, C. M. Brown, D. A. Neumann and J. R. Long, *J. Am. Chem. Soc.*, 2006, **128**, 16876–16883; (*b*) M. Dincă, W. S. Han, Y. Liu, A. Dailly, C. M. Brown and J. R. Long, *Angew. Chem., Int. Ed.*, 2007, **46**, 1419–1422; (*c*) K. Sumida, S. Horike, S. S. Kaye, Z. R. Herm, W. L. Queen, C. M. Brown, F. Grandjean, G. J. Long, A. Dailly and J. R. Long, *Chem. Sci.*, 2010, **1**, 184–191; (*d*) S. Biswas, M. Maes, A. Dhakshinamoorthy, M. Feyand, D. E. De Vos, H. Garcia and N. Stock, *J. Mater. Chem.*, 2012, **22**, 10200–10209.

19 R. Krishna and J. R. Long, *J. Phys. Chem. C*, 2011, **115**, 12941–12950.

20 S. S. Kaye, A. Dailly, O. M. Yaghi and J. R. Long, *J. Am. Chem. Soc.*, 2007, **129**, 14176–14177.

21 (*a*) J. A. Mason, K. Sumida, Z. R. Herm, R. Krishna and J. R. Long, *Energy Environ. Sci.*, 2011, **4**, 3030–3040; (*b*) R. Krishna and J. M. van Baten, *Phys. Chem. Chem. Phys.*, 2011, **13**, 10593–10616; (*c*) X. Peng, X. Cheng and D. Cao, *J. Mater. Chem.*, 2011, **21**, 11259–11270; (*d*) W. L. Queen, E. D. Bloch, C. M. Brown, M. R. Hudson, J. A. Mason,

L. J. Murray, A. J. Ramirez-Cuesta, V. K. Peterson and J. R. Long, *Dalton Trans.*, 2012, **41**, 4180–4187; (*e*) Z. R. Herm, R. Krishna and J. R. Long, *Microporous Mesoporous Mater.*, 2012, **151**, 481–487.

22 S. D. Ittel, L. K. Johnson and M. Brookhart, *Chem. Rev.*, 2000, **100**, 1169–1203.

23 (*a*) R. Krishna, B. Smit and S. Calero, *Chem. Soc. Rev.*, 2002, **31**, 185–194; (*b*) R. Krishna and J. M. van Baten, *Chem. Eng. J.*, 2007, **133**, 121–131.

24 D. R. Evans, T. Drovetskaya, R. Bau, C. A. Reed and P. D. W. Boyd, *J. Am. Chem. Soc.*, 1997, **119**, 3633–3634.

25 S. D. Pike, A. L. Thompson, A. G. Algarra, D. C. Apperley, S. A. Macgregor and A. S. Weller, *Science*, 2012, **337**, 1648–1651.

26 I. Castro-Rodriguez, H. Nakai, P. Gantzel, L. N. Zakharov, A. L. Rheingold and K. Meyer, *Inorg. Chem.*, 2003, **125**, 15734–15735.

27 (*a*) H.-F. Klein, R. Hammer, J. Gross and U. Schubert, *Angew. Chem., Int. Ed.*, 1980, **19**, 809–810; (*b*) B. Capelle, A. L. Beauchamp, M. Dartiguenave, Y. Dartiguenave and H. F. Klein, *J. Am. Chem. Soc.*, 1982, **104**, 3891–3897; (*c*) H. Butenschön, R. T. Kettenbach and C. Krüger, *Angew. Chem., Int. Ed.*, 1992, **31**, 1066–1068; (*d*) J. D. Jewson, L. M. Liable-Sands, G. P. A. Yap, A. L. Rheingold and K. H. Theopold, *Organometallics*, 1998, **18**, 300–305; (*e*) J. Foerstner, A. Kakoschke, R. Goddard, J. Rust, R. Wartchow and H. Butenschön, *J. Organomet. Chem.*, 2001, **617–618**, 412–422; (*f*) H.-F. Klein, R. Beck, U. Flörke and H.-J. Haupt, *Eur. J. Inorg. Chem.*, 2002, **2002**, 3305–3312; (*g*) O. Daugulis, M. Brookhart and P. S. White, *Organometallics*, 2003, **22**, 4699–4704; (*h*) H.-F. Klein, R. Beck, U. Flörke and H.-J. Haupt, *Eur. J. Inorg. Chem.*, 2003, **2003**, 1380–1387; (*i*) H. Wadepohl, *Anal. Sci.: X-Ray Struct. Anal. Online*, 2008, **24**, x225–x226.

28 Y. Kang, K.-i. Kim, S.-O. Kang, J. Ko, B. T. Heaton and J. V. Barkley, *J. Organomet. Chem.*, 1997, **532**, 79–82.

29 W. W. Brennessel, V. G. Young and J. E. Ellis, *Angew. Chem., Int. Ed.*, 2006, **45**, 7268–7271.